Spatial dispersion effects on the optical properties of a resonant Bragg reflector

L. Pilozzi and A. D'Andrea
Istituto di Metodologie Inorganiche e dei Plasmi, IMIP CNR, Rome, Italy

K. Cho
Graduate School of Engineering Science, Osaka University, Toyonaka, 560-8531 Japan
(Received 9 October 2003; revised manuscript received 20 January 2004; published 21 May 2004)

In the recent literature, aspects of exciton-radiation interaction in multilayers have been discussed from the viewpoint of microscopic nonlocal optical response. This renewed interest has also revived a long lasting debate about the problem of additional boundary conditions in dispersive samples. In the present paper, the semiclassical framework for studying self-consistently the radiation-matter interaction in a dispersive multilayer medium is briefly reviewed, and applied to the case of a one-dimensional (1D) cluster of quantum wells under Bragg conditions. The optical response is computed as a function of quantum well number N from the super-radiant regime (for rather small N values) to the 1D Bragg reflector limit ($N\rightarrow\infty$). The different contributions of the radiation-matter interaction to the optical response are discussed by Feenberg's decomposition of the polaritonic matrix. The polariton dispersion curves of a quantum well superlattice are computed and compared with the photonic dispersion curves due to the background dielectric function modulation. Finally, the modification of the photonic bands close to a resonance of the material system is discussed using selected numerical examples.

DOI: 10.1103/PhysRevB.69.205311 PACS number(s): 78.67.De, 71.36.+c, 71.35.Cc, 78.67.Pt

I. INTRODUCTION

Since the seminal paper of Yablonovich[1] a large number of papers has been devoted to the study of the optical properties of photonic crystals, obtained by modulating the spatial periodicity of materials with strongly different background dielectric values. An interesting property of these systems is the scalability of the photonic gap effect, which is a rather general property of diffraction in the regime of transparency[2] of the system. Nevertheless, this scalability is obtained by introducing a serious inconsistency in the model calculation; in fact, if only the dispersive effect of the light in the sample is taken into account, the Kramers-Kronig relationships cannot be satisfied by the dielectric function. On the other hand, since the optical properties of photonic crystals strongly depend on the dielectric contrast value, a huge enhancement of this value can be obtained for photon energies close to the resonances of the system, and this gain ''in some sense'' can compensate the lost scalability property.

The simplest photonic crystal showing resonant properties is the resonant Bragg reflector, obtained using multiple quantum wells (MQWs) at λ/2 separation. In this system the self-consistency between matter polarization and electromagnetic field leads to light mediated interactions between the QWs. This interaction changes the exciton-polariton self-energy and leads to a strong modification of the optical response of the system.

The optical theory for the case of finite quantum well number N has been developed, in terms of the super-radiant (SR) mode, in a number of papers.[3–9] The main result of these works is that there exists just one super-radiant mode which has a lifetime N times that of a single quantum well Γ_0, and the reflection coefficient for such a structure has been given in the form

$$R=\frac{(N\Gamma_0)^2}{(\omega-\omega_0)^2+(\gamma+N\Gamma_0)^2},$$

where γ is the nonradiative decay costant, and ω_0 the resonance energy.

Moreover, in the $N\rightarrow\infty$ limit, the dispersion equation, obtained by using the transfer matrix approach, has been given in the form[10,11]

$$\cos(Kd)=\cos(kd)-\Gamma_0\frac{\sin(kd)}{\omega-\omega_0-i\gamma}.$$

where d is the periodicity, K the wave vector of the system, and k the background wave vector of the photon.

Notice that both these formulas completely ignore the frequency dependence of the radiative damping, taking the polaritonic self-energy constant. This approximation is equivalent to the use of a local Lorentzian dielectric function which leads to the unphysical limit of a linear increase of the radiative decay. This effect was criticized by Ikawa and Cho,[12] who also underlined the importance of a self-consistent calculation in the nonlocal radiation-matter interaction for reaching the saturation effect of the radiative decay. Therefore, since the interpretation in terms of the SR mode becomes invalid in the $N\rightarrow\infty$ limit, it is considered necessary to establish a consistent picture connecting the two regimes for small and large N, and to derive the dispersion equation in the $N\rightarrow\infty$ limit. This transition from the super-radiant to the photonic crystal regime in a resonant Bragg reflector has been ascribed to the frequency dependence of radiative shift and width as a function of quantum well number N.[12] The calculation was performed taking into account the lowest Wannier exciton state for each quantum well. The numerical results show the building up of a large energy gap in the photonic crystal limit ($N\rightarrow\infty$), and the presence of a

reflection dip close to the resonant energy. In this paper we propose another picture of the evolution between the two regimes based on a particular decomposition of the polaritonic matrix.

In the optical response formulation described in the present paper, the driving field of the exciton polarization is the total field of the Maxwell equation, while in the framework used in Ref. 12 the transverse electromagnetic field is considered. We will point out that the two different choices give the same results, due to the self-consistency of the two methods. Moreover, the present method, based on the orthonormality property of the exciton envelope function in the ''site picture,'' is well suited also for two- (2D) and three-dimensional (3D) superlattices, where the transfer matrix method is no longer available, and it is completely equivalent to the rigorous approaches based on Bloch wave expansion.[13]

Finally, this renewed interest in the theory of the optical response in multiple quantum wells has also revived a long lasting debate about the problem of additional boundary conditions in dispersive samples.[14,15]

In the present work, the general procedure for computing the optical response in a cluster of N quantum wells is described in the framework of the self-consistent ''additional boundary condition (ABC) free theory.'' [12] The absorbance of the resonant Bragg system is computed for two different regimes, namely, (i) the super-radiance regime (for small clusters $N<80$), and (ii) the 1D resonant photonic crystal regime (for rather large clusters $N>300$), and discussed using selected numerical examples.

The total exciton-polariton susceptibility matrix, describing the well-well interaction, is studied by separating the interacting and noninteracting terms. In addition, the diagonal and off-diagonal contributions of the interacting part are singled out by the Feenberg method, which classifies all the irreducible terms of the well-well interaction.

Finally, the polariton dispersion curves for 1D resonant photonic crystals ($N\rightarrow\infty$) are computed, and the competition between the gap due to the polariton effect and that due to the normal dielectric background modulation of the multiple quantum well system is briefly discussed.

The paper is organized as follows. In Sec. II the semiclassical microscopic nonlocal self-consistent theory is presented, and the problem of the ABC is briefly addressed. In Sec. III this framework is adopted to obtain the optical response of a general multiple quantum well cluster of size N and the polariton dispersion curves in the limit of $N\rightarrow\infty$. Moreover, in the same section the polariton matrix decomposition is presented. In Sec. IV the optical properties and the dispersion curves for MQWs under the Bragg condition are computed and discussed using selected numerical examples. Section V contains concluding remarks.

II. NONLOCAL OPTICAL RESPONSE THEORY

It is well known that in the radiation-matter interaction the electromagnetic radiation field and the induced polarization of the material system must be determined self-consistently. In fact, the matter system will be dynamically polarized by the applied electromagnetic field, and in turn the induced polarization will determine the magnitude of the total electromagnetic field. Particular attention must be paid to the separation of the electromagnetic interaction between the ''matter'' and ''radiation'' Hamiltonians. The choice that embodies in the matter Hamiltonian direct and exchange interactions, and in the Maxwell equations (in their classical or quantum mechanical formulation[16]) the transverse radiation field, makes sense for separate systems. When the two systems are in interaction in the Coulomb gauge, one sensible choice is to consider the total electromagnetic field of the Maxwell equations as the driving field.

It is well known that for a dielectric tensor with spatial dispersion the Maxwell equations become integro-differential equations, and additional waves can also propagate in the medium in cubic crystals. This phenomenon usually requires additional boundary conditions (in addition to the normal Maxwell boundary conditions) in order to determine the optical response unambiguously. Three different procedures are usually used. (a) Phenomenological ABCs are used, based on microscopic consideration at the surface, along the lines of Pekar, Hopfield,[17] and many others.[18,19] (b) The Maxwell integro-differential equations are changed into higher (fourth-) order differential equations along the lines of Maradudin and Mills.[20,21] In this case, additional constraints come from the solution of the fourth-order differential equations, and therefore the ABCs are computed self-consistently from the dispersive dielectric function adopted. Finally, (c) the so called ABC free theory[22–24] is used, based on the Green function method, where the Maxwell integro-differential equations are trasformed into integral equations, and in this case the optical problem does not require ABCs at all for its solution.[25] Notice that the so called ''coherent theory'' proposed by Baslev *et al.*,[26] where the polarization and the Maxwell equations are solved on one footing, also belongs to this category. In conclusion, all the conditions that are necessary to unambiguously determine the electromagnetic problem are contained in the nonlocal microscopic theory[27] of the Maxwell equations, and in principle there is no reason to resort to additional boundary conditions.

Let us consider a material system composed of a cluster of N sites of nonoverlapping dispersive units, where $\varphi_\ell(\vec{r},Z)$ is the eigenfunction obtained by solving the unperturbed Hamiltonian of the ''matter,'' namely,

$$\hat{H}_0\varphi_\ell(\vec{r})=E_\ell\varphi_\ell(\vec{r}), \tag{1}$$

where $\ell=1,2,...,N$ is the site index.

In this site picture, the susceptibility is

$$\chi_{\alpha\beta}(\vec{r},\vec{r}';\omega)=\sum_\ell\left[\frac{\langle 0|\hat{P}_\alpha(\vec{r})|\ell\rangle\langle\ell|\hat{P}_\beta(\vec{r}')|0\rangle}{E_\ell-\hbar\omega-i\Gamma}+\frac{\langle 0|\hat{P}_\alpha(\vec{r}')|\ell\rangle\langle\ell|\hat{P}_\beta(\vec{r})|0\rangle}{E_\ell+\hbar\omega+i\Gamma}\right] \tag{2}$$

where $\alpha,\beta=x,y,z$ are the Cartesian coordinates and

$$\hat{P}(\vec{r}) = -i\frac{e}{m\omega}\sum_{\ell}\ \delta(\vec{r}-\vec{r}_{\ell})\vec{p}_n$$

is the dipole density operator.

The nonlocal induced polarization is

$$\vec{P}(\vec{r};\omega) = \int d\vec{r}'\,\vec{\vec{\chi}}(\vec{r},\vec{r}';\omega)\vec{E}(\vec{r}';\omega), \tag{3}$$

where $\vec{E}(\vec{r};\omega)$ is the electromagnetic field of the Maxwell equations. Therefore, eliminating the magnetic field and considering a nonmagnetic material, the Maxwell equation is

$$\vec{\nabla}\times\vec{\nabla}\times\vec{E}(\vec{r};\omega) + \frac{\omega^2}{c^2}\vec{E}(\vec{r};\omega) = \frac{\omega^2}{c^2}4\pi\vec{P}(\vec{r};\omega). \tag{4}$$

Notice that due to the earlier choice for the polarization [Eq. (3)], the exchange interaction must be subtracted from the matter Hamiltonian [Eq. (1)], because it appears also in the longitudinal part of the electromagnetic field (otherwise this contribution would be taken into account twice). Furthermore, in this case the use of a hydrogenic envelope function model[23,28] for describing the Wannier exciton in nanoparticles becomes an exact solution. In fact, not only the longitudinal-transverse splitting in a nanoparticle, but also the residual dipole-dipole interaction between nonoverlapping adjacent units, will be taken into account self-consistently by solving the Maxwell equation (4).

The electromagnetic field can be decomposed in two different ways. In the first one the electric field is decomposed into its transverse and longitudinal components:

$$\vec{E} = \vec{E}_T + \vec{E}_L$$

where $\vec{E}_L$ is the curl-free nonretarded Coulomb potential field:

$$\vec{E}_L(\vec{r};\omega) = \int d\vec{r}'\frac{\vec{\nabla}'\vec{\nabla}'\cdot\vec{P}(\vec{r}';\omega)}{|\vec{r}-\vec{r}'|},$$

while $\vec{E}_T$ is the solution of the Helmoltz equation, obtained by using the relationship

$$\vec{\nabla}\times\vec{\nabla}\times\cdots = [-\vec{\nabla}^2 + \vec{\nabla}\vec{\nabla}\cdot\cdots].$$

The second decomposition is obtained by writing the total electric field as

$$\vec{E} = \vec{E}_0 + \vec{E}_s,$$

where $\vec{E}_0$ is the general solution of the homogeneous problem associated with Eq. (4) [for $\vec{P}(\vec{r};\omega)=0$] and $\vec{E}_s$ is a special solution of the same equation.

From the knowledge of the homogeneous problem solution we can obtain the Green functions that satisfy the following heterogeneous equation:

$$\left[\vec{\nabla}\times\vec{\nabla}\times + \frac{\omega^2}{c^2}\right]\vec{\vec{G}}(\vec{r},\vec{r}';\omega) = \delta(\vec{r}-\vec{r}'), \tag{5}$$

and this allows us to change the integro-differential equation (4) into the following integral equation:

$$\vec{E}(\vec{r};\omega) = \vec{E}_0(\vec{r};\omega) - \frac{\omega^2}{c^2}\int d\vec{r}'\,\vec{\vec{G}}(\vec{r},\vec{r}';\omega) \times \int d\vec{r}''\,\vec{\vec{\chi}}(\vec{r}',\vec{r}'';\omega)\vec{E}(\vec{r}'';\omega), \tag{6}$$

which represents the Maxwell solution in implicit form.

In conclusion, the use of the Green function formalism does not require additional boundary conditions. The matter Hamiltonian, which takes into account longitudinal-transverse (LT) splitting, requires the use of the Maxwell transverse field for driving the polarization, while, in the case of a simple model Hamiltonian (like the hydrogenic one), it is simpler to use the total Maxwell electromagnetic field in order to take into account the dipole-dipole interaction also. We will adopt this latter choice in the whole paper.

III. POLARITONS IN MULTIPLE QUANTUM WELLS

The exciton envelope function in a multiple quantum well system or superlattice requires different descriptions according to the overlap values between next-neighbor quantum wells. For nonoverlapping excitons in different quantum wells, the orthogonality between exciton envelope functions in different sites can be used. In this case two different mechanisms can delocalize the exciton-polariton in the whole sample. For a very large distance between the well and its next neighbors, as for MQWs under the Bragg condition, the delocalization is due to the retarded transverse electric field, while for a very small distance, and under non-normal incidence, the nonradiative longitudinal electric field can also contribute via the dipole-dipole interaction.

A. Optical response of a cluster of *N* quantum wells

Let us consider a cluster of N semiconductor quantum wells as shown in Fig. 1. The material system has cubic symmetry, and we can choose Cartesian coordinates with the Z axis along the growth direction, and, by using the cylindrical symmetry of the quantum wells, we can adopt mixed coordinates $(\vec{K}_{\parallel},Z)$ for the center-of-mass motion of the Wannier exciton. In this case the 2D-exciton envelope functions are $\varphi_{\ell}(\vec{r},Z)e^{i\vec{K}_{\parallel}\cdot\vec{R}_{\parallel}}/\sqrt{S}$ with variationally determined eigenvalues

$$E_{\ell}(K_{\parallel}) = E_{\rm gap} - E_{1S}(\ell) + \frac{\hbar^2}{2M}K_{\parallel}^2.$$

The dielectric tensor, composed of local and nonlocal contributions, is

$$\varepsilon^{\alpha,\beta}(Z,Z';\omega) = [\varepsilon_b\delta(Z-Z') + 4\pi\chi^{\alpha}(Z,Z';\omega)]\delta_{\alpha,\beta}, \tag{7}$$

where $\alpha,\beta = x,y,z$, ε_b is the bulk dielectric constant, and taking into account the correspondence $T\rightarrow X$, $L\rightarrow Y$, and $Z\rightarrow Z$ we obtain the dielectric tensor for the three different polarizations.

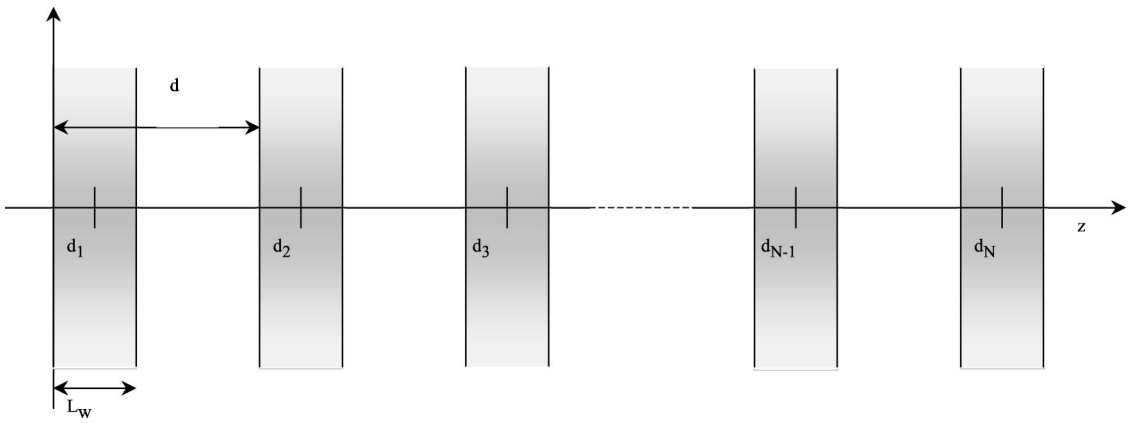

FIG. 1. Material system under study: cluster of N quantum wells.

From Eq. (2) the susceptibility is

$$4\pi\chi_\alpha(Z,Z';\omega)=\sum_\ell S_0^\alpha(\omega)\left[\frac{\varphi_\ell^*(Z)\varphi_\ell(Z')}{E_\ell(K_\parallel)-\hbar\omega-i\Gamma_\ell}+\frac{\varphi_\ell(Z)\varphi_\ell^*(Z')}{E_\ell(K_\parallel)+\hbar\omega+i\Gamma_\ell}\right], \tag{8}$$

where $S_0^\alpha(\omega)=4\pi g_\alpha E_k e^2\hbar^2/(\hbar\omega)^2 m_e$, $E_K=2|p_{vc}|^2/m_e$ is the Kane energy of the interband (valence→condition) transition, and g_α is the multiplicity of the state (for the heavy-hole exciton $g_\alpha=1/2$ for T and L polarization, while for the light-hole exciton $g_\alpha=1/6$ for T and L polarization and $g_\alpha=2/3$ for Z polarization).

Let us consider the heavy-hole exciton, where the Z component of the electric dipole moment is zero $[S_0^\alpha(\omega)=0]$. If we take the same values for the dielectric constant of the background in quantum wells and in barriers (ε_b), the Maxwell equations are greatly simplified. In fact, for $\alpha=x,y$ and $\vec{K}_\parallel\equiv k_x\hat{i}$, the integro-differential Maxwell equation becomes

$$\left[\frac{d^2}{dZ^2}+K_z^2\right]E_\alpha(Z;\omega)=-\frac{\omega^2}{c^2}\int\tilde{\chi}_\alpha(Z,Z';\omega)E_\alpha(Z';\omega)dZ', \tag{9}$$

where $K_z=[K^2-K_\parallel^2]^{1/2}$ and $K=(\omega/c)\sqrt{\varepsilon_b}$. For L polarization the electric field Z component is $E_z(Z;\omega)=i(K_\parallel/K_z^2)\times(dE_x(Z;\omega)/dZ)$ and the susceptibilities in Eq. (9) are $\tilde{\chi}_y(Z,Z';\omega)\equiv\chi_y(Z,Z';\omega)$ and $\tilde{\chi}_x(Z,Z';\omega)\equiv(K_z^2/K^2)\chi_x(Z,Z';\omega)$ for T and L polarizations, respectively.

The solution proceeds by computing the Green function

$$\left[\frac{d^2}{dZ^2}+K_z^2\right]G(Z,Z';\omega)=\delta(Z-Z'), \tag{10}$$

where the "bulk" Green function is $G(Z,Z';\omega)=e^{iK_z|Z-Z'|}/(2iK_z)$.

The formal solution of Eq. (9) is given in the integral form

$$E_\alpha(Z;\omega)=E_\alpha^0(Z;\omega)-\frac{\omega^2}{c^2}\int dZ'G(Z,Z';\omega)\times\int dZ''\chi(Z',Z'';\omega)E_\alpha(Z'';\omega),$$

and a great simplification of the problem comes from the fact that the kernel of this equation is separable with respect to the spatial coordinates (degenerate kernel), and in the rotating-wave approximation (RWA) can be written

$$\chi_\alpha(Z,Z';\omega)=\sum_\ell\chi_\ell^\alpha(\omega)\varphi_\ell^*(Z)\varphi_\ell(Z').$$

This property allows us to rewrite the solution as

$$E_\alpha(Z;\omega)=E_\alpha^0(Z;\omega)-\frac{\omega^2}{c^2}\sum_\ell\chi_\ell^\alpha(\omega)I_\ell^\alpha(\omega)G_\ell(Z;\omega), \tag{11}$$

where $G_\ell(Z;\omega)=\int dZ'G(Z,Z';\omega)\varphi_\ell(Z')$ and $I_\ell^\alpha(\omega)=\int dZ'\varphi_\ell(Z')E_\alpha(Z';\omega)$, which changes the Maxwell integral equation into a system of coupled linear algebraic equations.

In fact, by applying the operator $\int dZ\varphi_\ell(Z)$ to Eq. (11), we recover a self-consistent solution of the electromagnetic field,

$$I_\ell^\alpha(\omega)=\sum_{\ell'}(\vec{\vec{D}}_\alpha^{-1})_{\ell,\ell'}I_{\ell'}^0(\omega), \tag{12}$$

where the polariton matrix $\vec{\vec{D}}_\alpha(\omega)$ is

$$(\vec{\vec{D}}_\alpha)_{\ell\ell'}(\omega)=\delta_{\ell,\ell'}+\frac{\omega^2}{c^2}\chi_\ell^\alpha(\omega)M_{\ell\ell'}^\alpha(\omega) \tag{13}$$

and $M_{\ell\ell'}^\alpha(\omega)=\int dZdZ'\varphi_\ell^*(Z)G(Z,Z';\omega)\varphi_{\ell'}(Z')$ while $I_\ell^{0,\alpha}(\omega)=\int dZ\varphi_\ell^*(Z)E_\alpha^0(Z;\omega)$ are the known quantities.

The matrix $\vec{\vec{D}}_\alpha(\omega)$ is $N\times N$, and the diagonal elements embody the self-energy of the exciton located in the quantum well of the ℓth site of the sample, while the off-diagonal elements contain the interaction between wells in different sites ($\ell\neq\ell'$).

The homogeneous solution for $Z\to-\infty$ is

$$E_\alpha^0(Z;\omega)=A_\alpha e^{iK_zZ}+B_\alpha e^{-iK_zZ}=A_\alpha e^{iK_zZ} \tag{14}$$

with $A_\alpha=1$, due to the normalization, and $B_\alpha=0$ if we consider the same background dielectric constant in the whole space. Notice that in our procedure calculation we have used the ''bulk'' Green function solution for each zone of the sample with the same background dielectric constant; afterward we impose the Maxwell boundary condition at the surfaces. A different procedure requires the use of the Green function available for the whole range of Z values;[22] in this second case the optical response is computed as the limiting value ($Z\to\pm\infty$) of the electric field. The first option is more flexible than the second one, because it separates the Maxwell solution in each slab from the matching between different slabs of the layered system, and it will be adopted in the present calculation.

If we take d_ℓ as the distance of the ℓ site from the $Z=0$ surface, and $\varphi_\ell^0(K_z)$ is the Fourier transform of the exciton envelope function evaluated for $\vec{r}=0$ and computed with respect to the center of symmetry of the ℓth quantum well, the quantity G_ℓ for $Z\to-\infty$ is

$$G_\ell(Z\to-\infty;\omega)=\lim_{Z\to-\infty}[e^{-iK_zZ}\varphi_\ell^0(K_z)e^{iK_zd_\ell}/(2iK_z)]. \tag{15}$$

Therefore, the total electric field is

$$E_\alpha(Z\to-\infty;\omega)=\lim_{Z\to-\infty}[e^{iK_zZ}-e^{-iK_zZ}\Delta^\alpha(Z;\omega)], \tag{16}$$

where the quantity

$$\Delta^\alpha(Z\to-\infty;\omega)=\frac{\omega^2}{c^2}\sum_{\ell\ell'}\frac{\chi_\ell^\alpha(\omega)}{2iK_Z}e^{iK_Z(d_{\ell'}+d_\ell)}\varphi_\ell^0(K_Z)\times(\vec{\vec{D}}_\alpha^{-1})_{\ell\ell'}(\omega)\varphi_{\ell'}^0(K_Z) \tag{17}$$

is the field polarization on the surface, and in this case is also the reflection amplitude of the system.

For $Z\to+\infty$,

$$G_\ell(Z\to\infty;\omega)=\lim_{Z\to\infty}[e^{iK_zZ}\varphi_\ell^0(-K_z)e^{-iK_zd_\ell}/(2iK_z)]$$

and

$$\Delta^\alpha(Z\to\infty;\omega)=\frac{\omega^2}{c^2}\sum_{\ell\ell'}\frac{\chi_\ell^\alpha(\omega)}{2iK_Z}e^{iK_Z(d_{\ell'}-d_\ell)}\varphi_\ell^0(-K_Z)\times(\vec{\vec{D}}_\alpha^{-1})_{\ell\ell'}(\omega)\varphi_{\ell'}^0(K_Z) \tag{18}$$

and the electric field is

$$E_\alpha(Z\to\infty;\omega)=\lim_{Z\to\infty}e^{iK_zZ}[1-\Delta^\alpha(Z\to\infty;\omega)], \tag{19}$$

where the quantity in the square brackets is the transmission amplitude of the system.

Finally, the absorption is given by

$$A_\alpha(\omega)=1-|\Delta^\alpha(Z\to-\infty;\omega)|^2-|1-\Delta^\alpha(Z\to\infty;\omega)|^2. \tag{20}$$

Now, if we consider the vacuum-bulk dielectric discontinuity on the surface at $Z=0$, the homogeneous solution on the surface is the same as Eq. (14), but with $B_\alpha\neq0$.

Therefore

$$G_\ell(Z=0;\omega)=\lim_{Z\to0^+}[e^{-iK_zZ}\varphi_\ell^0(K_z)e^{iK_zd_\ell}/(2iK_z)]$$

and, the total electric field on the surface is

$$E_\alpha(Z\to0^+;\omega)=\lim_{Z\to0^+}A_\alpha\{e^{iK_zZ}-e^{-iK_zZ}\Delta^\alpha(Z;\omega)\}, \tag{21}$$

where the polarization field on the surface is the quantity given in Eq. (17).

The electric field in the vacuum side ($Z<0$) is

$$E_\alpha(Z;\omega)=e^{iq_zZ}+r_\alpha e^{-iq_zZ}$$

where $q_z=[\omega^2/c^2-K_\parallel^2]^{1/2}$ and, by imposing the Maxwell's boundary conditions at the surface ($Z=0$), we obtain the reflectivity for $\alpha=y\Rightarrow S$ and $\alpha=x\Rightarrow P$:

$$r_\alpha(\omega)=\frac{r_\alpha^0-\Delta^\alpha(\omega)}{1-r_\alpha^0\Delta^\alpha(\omega)} \tag{22}$$

where r_α^0 is the unperturbed reflectivity at the surface, and the amplitudes $A_\alpha(\omega)$ are

$$A_y(\omega)=\frac{2q_z}{q_z+K_z}[1-r_S^0\Delta^y(\omega)]^{-1},$$

$$A_x(\omega)=\frac{2\varepsilon_bK_z}{\varepsilon_bq_z+K_z}[1-r_p^0\Delta^x(\omega)]^{-1}. \tag{23}$$

The diagonal elements of the polariton matrix have the simple form (in the RWA)

$$D_{\ell,\ell}^\alpha(\omega)=1+\frac{\omega^2}{c^2}\chi_\ell^\alpha(\omega)M_{\ell,\ell}^\alpha(\omega)$$

$$=\frac{E_{\rm gap}-E_{\rm ex}(\ell)+(\hbar^2/2M)K_\parallel^2-\hbar\omega-i\Gamma_\ell+(\omega^2/c^2)S_0^\alpha M_{\ell,\ell}(\omega)}{E_{\rm gap}-E_{\rm ex}(\ell)+(\hbar^2/2M)K_\parallel^2-\hbar\omega-i\Gamma_\ell} \tag{24}$$

and $\Sigma_{\mathrm{pol}}(\omega)=\Sigma'(\omega)+i\Sigma''(\omega)=(\omega^2/c^2)S_0^{\alpha}M_{\ell,\ell}(\omega)$ is the polariton self-energy for the single quantum well. For the 2D exciton envelope function

$$\varphi_{\ell}(Z)=N_{\ell}\left[\cos\left(\frac{\pi}{L}(Z-d_{\ell})\right)\right]^2$$

the diagonal elements are

$$M_{\ell,\ell}(\omega)=\mathrm{Re}[M_{\ell,\ell}(\omega)]+\frac{1}{2iK_z}[\varphi_{\ell}^0(K_z)]^2$$

while the off-diagonal ones, embodying the interaction between different quantum wells are $M_{\ell\neq\ell'}(\omega)=(1/2iK_z)\varphi_{\ell}^0(K_z)\varphi_{\ell'}^0(K_z)e^{iK_z|d_{\ell}-d_{\ell'}|}$.

The quantity of Eq. (17) is

$$\Delta^{\alpha}(\omega)=\frac{\omega^2}{c^2}\sum_{\ell}\chi_{\ell}^{\alpha}(\omega)\frac{[\varphi_{\ell}^0(K_z)]^2}{2iK_z}\times\sum_{\ell'}[\vec{\vec{D}}_{\alpha}^{-1}(\omega)]_{\ell,\ell'}e^{iK_z(d_{\ell}+d_{\ell'})}. \tag{25}$$

In order to disentangle in this quantity the single quantum well contribution from the total interaction, let us decompose the matrix of Eq. (24) as a sum of its diagonal and off-diagonal elements:

$$D_{\ell,\ell'}(\omega)=D_{\ell,\ell}(\omega)\delta_{\ell,\ell'}+D_{\ell,\ell'}(\omega)(1-\delta_{\ell,\ell'})=A_{\ell,\ell'}+B_{\ell,\ell'};$$

therefore, $\vec{\vec{D}}=\vec{\vec{A}}+\vec{\vec{B}}=\vec{\vec{A}}[\vec{\vec{I}}+\vec{\vec{A}}^{-1}\vec{\vec{B}}]=\vec{\vec{A}}\vec{\vec{C}}$, where the $\vec{\vec{A}}$ matrix is diagonal, and its nonzero elements are the single quantum well contribution to the surface electric field; the $\vec{\vec{C}}$ matrix has one along the diagonal, while its off-diagonal elements are the polariton well-well interactions. Since $\vec{\vec{D}}^{-1}=\vec{\vec{C}}^{-1}\vec{\vec{A}}^{-1}$ and the matrix elements are

$$(\vec{\vec{D}}^{-1})_{\ell,\ell'}=\sum_{\ell''}(\vec{\vec{C}}^{-1})_{\ell,\ell''}(\vec{\vec{A}}^{-1})_{\ell'',\ell'}=\sum_{\ell''}(\vec{\vec{C}}^{-1})_{\ell,\ell''}(D_{\ell',\ell'})^{-1}\delta_{\ell'',\ell'}$$

from Eq. (25) we obtain

$$\Delta^{\alpha}(\omega)=\frac{\omega^2}{c^2}\sum_{\ell,\ell'}\chi_{\ell}^{\alpha}(\omega)\frac{[\varphi_{\ell}^0(K_z)]^2}{2iK_z}(\vec{\vec{C}}^{-1})_{\ell,\ell'}(D_{\ell',\ell'})^{-1}\times e^{iK_z(d_{\ell}+d_{\ell'})}. \tag{26}$$

For $\ell=\ell'$ the matrix elements $(\vec{\vec{C}}^{-1})_{\ell,\ell'}$ can be decomposed into irreducible contributions by Feenberg's expansion,[29]

$$(\vec{\vec{C}}^{-1})_{\ell,\ell}=\frac{C^{\ell}}{C}=\frac{1}{c_{\ell,\ell}}\left[1-\frac{F^{\ell}}{C}\right],$$

where c_{ij} are the elements of the $\vec{\vec{C}}$ matrix, C is its determinant, and C^{ℓ} is the determinant of the minor of $\vec{\vec{C}}$ obtained by suppressing the ℓth row and column; F^{ℓ} is the Feenberg irreducible decomposition of the matrix, namely,

$$C=c_{\ell,\ell}C^{\ell}-\sum_{j\neq\ell}c_{\ell,j}c_{j,\ell}C^{\ell,j}+\sum_{j\neq\ell}\sum_{\substack{i\neq\ell\\ i\neq j}}c_{\ell,j}c_{j,i}c_{i,\ell}C^{\ell,j,i}-\cdots=c_{\ell,\ell}C^{\ell}+F^{\ell},$$

where in our case $c_{\ell,\ell}=1$, and $C^{\ell,i,j,\cdots}$ is the determinant of the minor of $\vec{\vec{C}}$ obtained by suppressing the $(\ell,i,j,\ldots)$th rows and columns.

Finally, the quantity $\Delta^{\alpha}(\omega)$ can be decomposed into diagonal and off-diagonal components, and, moreover, in the diagonal component we can single out the contribution of the noninteracting quantum wells, namely,

$$\begin{aligned}\Delta^{\alpha}(\omega)=&\frac{\omega^2}{c^2}\sum_{\ell}\sum_{\ell'\neq\ell}\chi_{\ell}^{\alpha}(\omega)\frac{[\varphi_{\ell}^0(K_z)]^2}{2iK_z}(\vec{\vec{C}}^{-1})_{\ell,\ell'}\\&\times(D_{\ell',\ell'}^{\alpha})^{-1}e^{iK_z(d_{\ell}+d_{\ell'})}\\&-\frac{\omega^2}{c^2}\sum_{\ell}\chi_{\ell}^{\alpha}(\omega)\frac{[\varphi_{\ell}^0(K_z)]^2}{2iK_z}[F_{\alpha}^{\ell}(\omega)/C(\omega)]\\&\times[D_{\ell,\ell}^{\alpha}(\omega)]^{-1}e^{i2K_zd_{\ell}}\\&+\frac{\omega^2}{c^2}\sum_{\ell}\chi_{\ell}^{\alpha}(\omega)\frac{[\varphi_{\ell}^0(K_z)]^2}{2iK_z}[D_{\ell,\ell}^{\alpha}(\omega)]^{-1}e^{i2K_zd_{\ell}}.\end{aligned} \tag{27}$$

Notice that the third term on the right side is the interaction between the electromagnetic field and N noninteracting quantum wells located at ℓ sites of the sample, namely,

$$\Delta_S^{\alpha}(\omega)=\sum_{\ell}\Delta_{\ell}^{\alpha}(\omega)=\frac{\omega^2}{c^2}\sum_{\ell}\chi_{\ell}^{\alpha}(\omega)\frac{[\varphi_{\ell}^0(K_z)]^2}{2iK_z}[D_{\ell,\ell}^{\alpha}(\omega)]^{-1}e^{i2K_zd_{\ell}}. \tag{28}$$

This contribution is essentially a ''scale factor'' of the cluster; in fact, its value scales as the sum of the single-well contributions.

The second term of Eq. (27) embodies diagonal polariton effects not reducible to the noninteracting contribution of Eq. (28). Finally, the first term is an off-diagonal term connecting a well with a different well of the system. In conclusion, the decomposition of $\Delta^{\alpha}(\omega)$ is

$$\Delta^{\alpha}(\omega)=\Delta_{\mathrm{OD}}^{\alpha}(\omega)+\Delta_D^{\alpha}(\omega)+\Delta_S^{\alpha}(\omega). \tag{29}$$

The analysis of the evolution with N of the square modulus of the quantities quoted in Eq. (29) for a cluster of N identical quantum wells under the Bragg condition (see Fig. 1) is shown in Fig. 2. The physical parameter values used in the

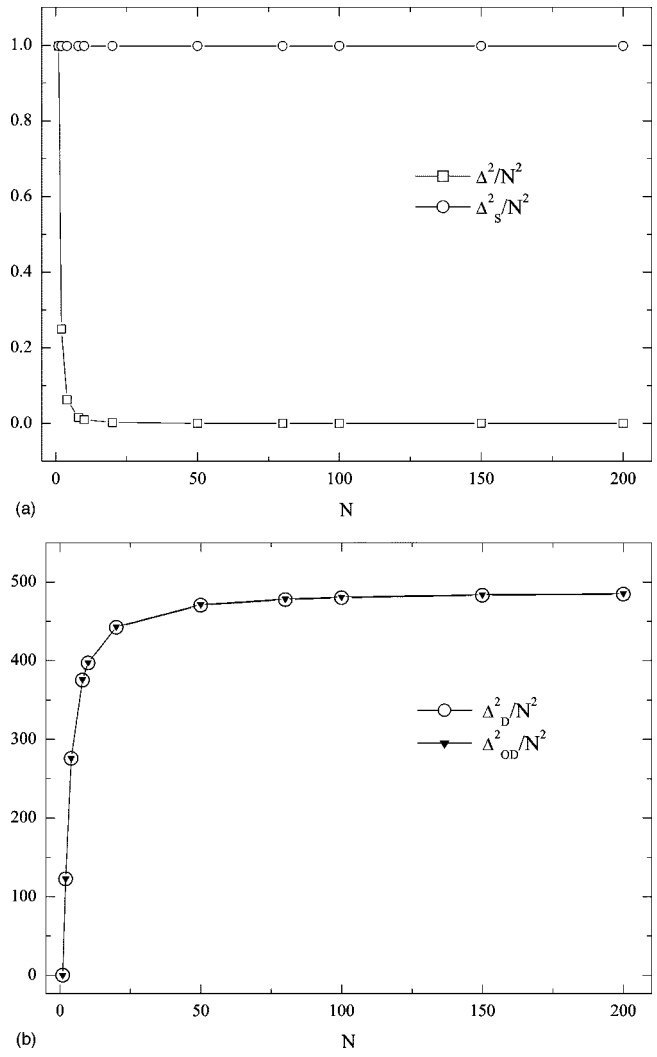

FIG. 2. Square modulus of polarization field on the surface, performed at the energy of exciton resonance as a function of the quantum well number N and normalized to the square of the quantum well number itself. (a) Circles, single quantum well contribution Δ_S^2/N^2; squares, total term $\Delta^2/N^2=(\Delta_S+\Delta_D+\Delta_{\mathrm{OD}})^2/N^2$. (b) Diagonal and off-diagonal terms $\Delta^2_{D/\mathrm{OD}}/N^2$.

calculation are given in Table I. These values are chosen very close to those of the AlGaAs/GaAs(001) system. Moreover, for describing the radiation-matter interaction of the system, a very small nonradiative homogenous broadening is taken ($\Gamma_{\mathrm{NR}}=10^{-12}$ eV).

The calculation is performed at the energy of the exciton resonance and the values are normalized to the square of the quantum well number itself. Notice that the noninteracting quantum well term $\Delta_S^{\alpha}(\omega)$ [Eq. (28)] is constant since it scales with N as discussed before [circles in Fig. 2(a)]. Under resonance condition, the diagonal term $\Delta_D^{\alpha}(\omega)$, subtracted from the noninteracting well contribution, has the same value as the off-diagonal term as is shown in Fig. 2(b), and these two quantities reach their asymptotic values very fast, underlining that the Bragg phase conditions are reached for a rather small number of quantum wells (about $N=20$). Finally, the electric field at the surface decreases with a $1/N^2$ behavior as expected [squares in Fig. 2(a)].

B. Polariton dispersion curves for 1D resonant photonic crystal

Let us consider a 1D lattice as shown in Fig. 1 for $N\rightarrow\infty$ where the dielectric function modulation is due to the quantum wells and barriers.

The polariton dispersion curve is computed by imposing the boundary conditions at the quantum well surfaces located at the site 1, and the periodicity condition as for the normal photonic Kronig and Penney model. We observe that the electric field [see, for instance, Eq. (14)] computed at the well surfaces in the site 1 and that in the site ℓ differ only by a phase translation due to the Fourier transform of the exciton envelope function; all the other quantities depending on the spatial dispersion effect, [namely, the self-energy and the z-dependent function $G_\ell(Z,\omega)$] are site independent due to the $|Z-Z'|$ difference present in the ''bulk'' Green function. After some algebra, the polariton dispersion curves are given by the real part of the following complex equation:

$$\begin{aligned}\cos(Kd)=\frac{(k_z+q_z)^2}{8q_zk_z\varepsilon}(e^{iq_z(d-L_w)}\{e^{ik_zL_w}[\varepsilon-i\Sigma''(\omega)]\\ -r_0^2[\varepsilon+i\Sigma''(\omega)]e^{-ik_zL_w}-2i\Sigma''(\omega)r_0\}\\ +e^{-iq_z(d-L_w)}\{[\varepsilon+i\Sigma''(\omega)]e^{-ik_zL_w}\\ -r_0^2e^{ik_zL_w}[\varepsilon-i\Sigma''(\omega)]+2i\Sigma''(\omega)r_0\})\end{aligned}\quad(30)$$

with, $r_0=(k_z-q_z)/(k_z+q_z)$ and $\hbar\omega_0-\hbar\omega-i\Gamma_1+\Sigma(\omega)=\varepsilon+i\Sigma''(\omega)$, where $\Sigma(\omega)=\Sigma'(\omega)+i\Sigma''(\omega)$ is the polariton self-energy of a single quantum well.

Finally, for the special case $q_z=k_z$ the system is greatly simplified:

$$\varepsilon\cos(Kd)=\varepsilon\cos(q_zd)+\Sigma_1''(\omega)\sin(q_zd),\quad(31)$$

and, if we neglect the exciton contribution to the dielectric susceptibility, we recover the photonic Kroening and Penney result for dielectric constant modulation, namely,

$$\begin{aligned}\cos(Kd)=\cos(k_zL_w)\cos[q_z(d-L_w)]\\ -\frac{(k_z^2+q_z^2)}{2q_zk_z}\sin(k_zL_w)\sin[q_z(d-L_w)].\end{aligned}\quad(32)$$

The polariton dispersion curves are computed by taking the same dielectric constant value for wells and barriers (Table I); the numerical results are given in Fig. 3, where the dispersion curve behavior at the band edges is also shown in an expanded scale in Figs. 3(b) and 3(c). The contribution due to the exciton-polariton is the appearance of a third curve at $\hbar\omega_0+\Sigma'(\omega)$, where $\Sigma'(\omega)$ is the radiative shift due to the exciton-polariton self-energy of a single well. This curve drops in the middle of the two dispersion curves present also

TABLE I. Physical parameter values.

$\varepsilon_b=12.6$	$L_W=8$ nm
$\hbar\omega_0=1.5152$ eV	$d_{\ell+1}-d_\ell=\lambda(\omega_0)/2$
$\Sigma''(\omega_0)=0.033$ meV	$d_1=\lambda(\omega_0)/2$

in the dielectric photonic Kronig-Penney model. In Fig. 3(d) the disappearance of the exciton-polariton radiative shift at the band edge (π/d) is also shown.

In the present case, where the background dielectric constants are the same for wells and barriers, all the dispersion curves are due to the interplay between the background dielectric constant and the dispersive part of the nonlocal exciton dielectric function. This dispersive component is large at the exciton resonant energy, while for the higher energies we observe the appearance of higher energy narrow gaps due to the small value of the real part of the exciton dielectric function, and obviously the disappearance of the central dispersion curve. Notice that for the condition of Eq. (30) the dispersion curves of a 1D resonant photonic crystal look the same as those of the photon bulk dispersion [see Fig. 3(a)], except for the appearance of the central curve; in reality, great differences appear in an expanded scale at the high symmetry points, as shown in Figs. 3(b) and 3(c) for the resonant and the off-resonant energy, respectively. The photon bulk dispersion curves cross the boundary of the Brillouin zone at $n\hbar\omega_0$ due to the Bragg condition as expected [see Figs. 3(b) and 3(c)].

These results underline the importance of the use of a well behaved dielectric function also for photon energy very far from the resonance energies of the system.

IV. RESULTS AND DISCUSSION

The reflectivity and absorbance spectra as a function of the QW number N, for the system given in Fig. 1, show three different behaviors, namely, (i) the super-radiant regime for $2<N<80$, (ii) the 1D resonant Bragg reflector for $80<N<500$, and (iii) the 1D resonant photonic crystal limit (for $N\rightarrow\infty$).

A. Super-radiant regime vs 1D Bragg reflector

The reflectivity spectra, computed self-consistently, for different quantum well numbers from the super-radiant to the 1D Bragg reflector behavior are shown in Fig. 4(a). The characteristic line shape modification from Lorentzian- to Bragg-reflector-like, due to the increase of the quantum well number, is clearly observed.

The half width at half maximum (HWHM) of the reflectivity as a function of quantum well number ($N=1-500$) is given in Fig. 4(b). The behavior of the curve is usually explained by taking into account that three different zones are observed, namely, (i) in zone I the linear behavior is connected with the super-radiant regime, while (ii) zone II is the transition zone, where the super-radiant mode redistributes its radiative interaction among all the levels of the system, and, finally, (iii) zone III is the saturation zone, where the reflectivity shows the Bragg reflector behavior [see Fig. 4(a)]. Notice that this interpretation is not exaustive of all the phenomena involved in the optical response of these systems, as we will point out in the present work.

In order to go a bit deeper into understanding the exciton-polariton behavior in Bragg MQWs, let us consider the absorbance of the system, given in Eq. (20), as a function of well number.

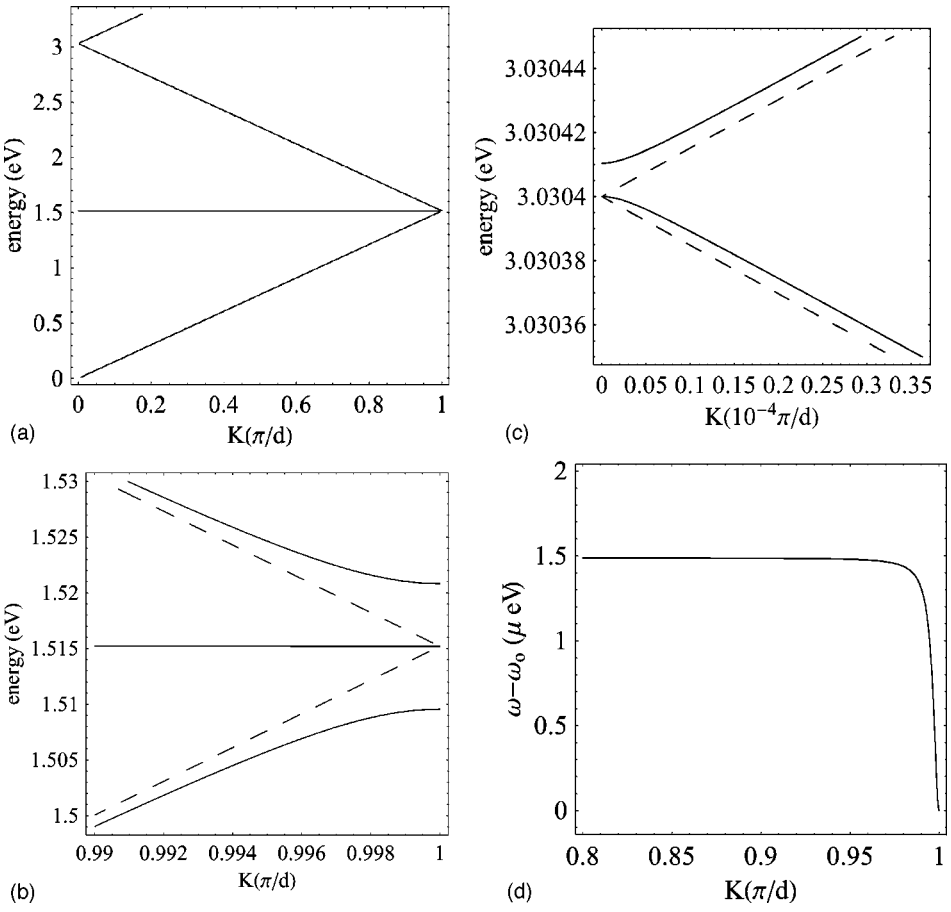

FIG. 3. (a) Polariton dispersion curves of a 1D resonant photonic crystal. (b), (c), (d) polariton curves in expanded scales. In (b),(c) the dashed line is the photonic curve obtained by neglecting the exciton contribution.

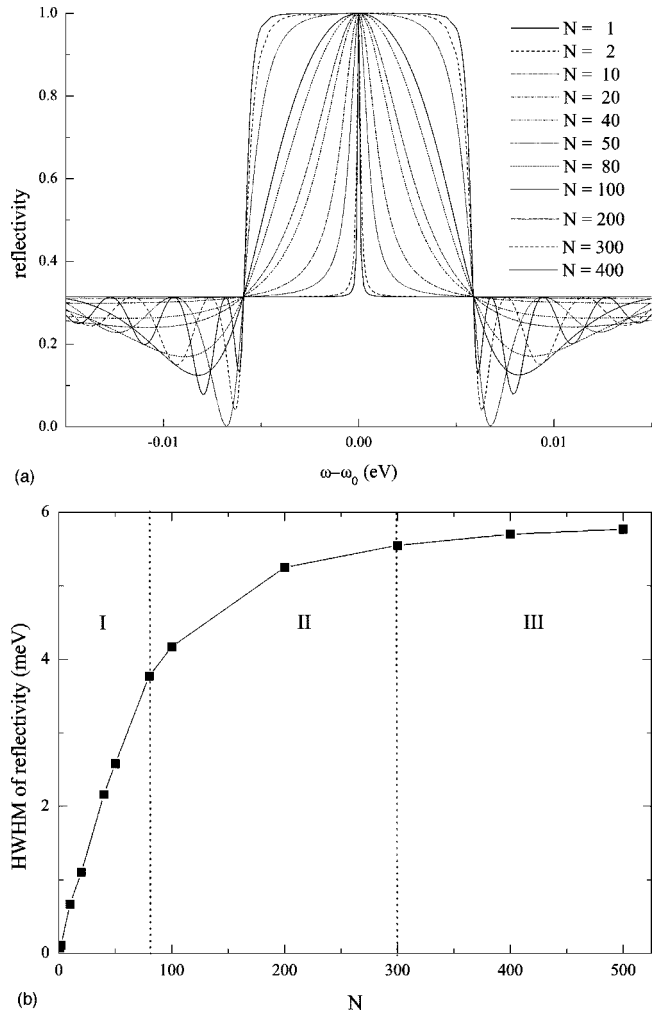

FIG. 4. (a) Reflectivity spectrum for a 1D array of N identical quantum wells for $1<N<400$. (b) Half width at half maximum of the reflectivity as a function of quantum well number.

In Fig. 5 the absorbance for $N=1-80$ is shown. We observe the presence of only one absorbance peak whose area (total absorbance) remains constant on increasing the N value, and this assures us that it is the only bright mode of the system. Furthermore, the linear behavior of the broadening of the absorbance peaks [see Fig. 6(a)] is usually interpreted as a fingerprint of super-radiant manifestation.

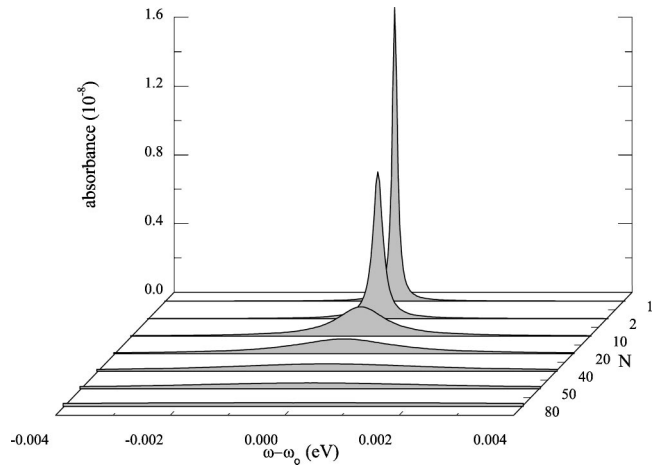

FIG. 5. Absorbance as a function of quantum well number in the super-radiant regime: $1<N<80$.

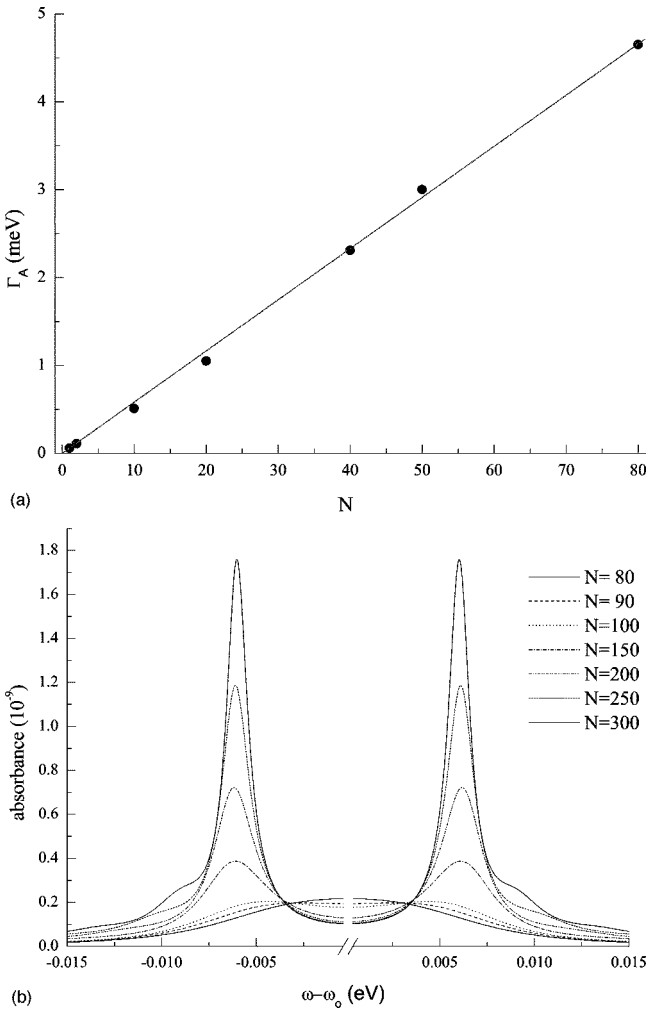

FIG. 6. (a) Broadening of the absorbance peaks Γ_A for $1<N<80$. (b) Absorbance of the system for $80<N<300$.

Above this limit value ($N>80$), the absorbance peak splits into two sidebands appearing at the border of the reflectivity ''stop band'' of the system [see Fig. 6(b)]. Since the so called ''dark modes'' become bright,[12] in coincidence with their energies the optical spectrum shows additional dips, which strongly modify the ''stop band'' for energy values close to the resonance energy. In Fig. 7 the energy position of the reflectance dips, computed in the transition region [zone II of Fig.4 (b)] as a function of quantum well number, is reported, and by increasing the well number N, the energy spreading of the curves clearly underlines the switching on of the radiation–dark mode interaction. In principle, this energy spreading should be as large as the radiative shift of a single quantum well, and the modes are localized between $\hbar\omega_0+\Sigma'(\omega_0)$ and $\hbar\omega_0$, as will be discussed in the next section.

In Fig. 8 some of the absorbance peaks are shown for the case $N=200$, and also the reflectivity and transmittivity curves are reported in the same pictures. The half width at

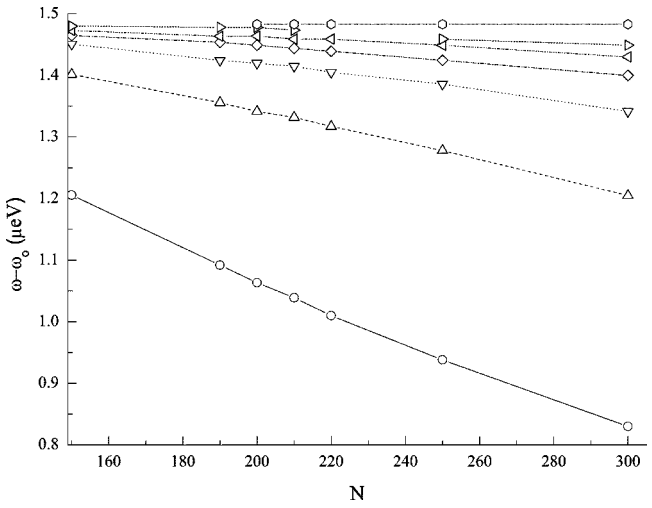

FIG. 7. Energy position of the reflectance dips computed in the transition region.

half maximum of the absorbance peaks decreases from about 25 times the nonradiative broadening to the nonradiative broadening value for a photon energy that ranges from $\hbar\omega_0$, to $\hbar\omega_0+\Sigma'(\omega_0)$. This effect is connected with the conversion of the polariton self-energy of the system from real to imaginary character on approaching the resonance energy. Therefore, a large part of the $(N-1)$ electromagnetic modes of the system are embodied in the peaks close to this energy. The same behavior is also observed for reflectance and transmittance peaks.

These results clearly underline that, for a large 1D cluster of quantum wells, the exciton-photon interaction redistributes its intensity among all the N states of the system, and the exciton-polariton self-energy, due to the well-well interaction, changes from a purely imaginary contribution for the super-radiant regime to a real contribution for a 1D resonant photonic crystal.

Finally, in the next section the optical properties of a MQWs under Bragg conditions will be discussed for the 1D resonant photonic crystal limit $(N\rightarrow\infty)$.

B. 1D resonant photonic crystals

Let us consider a 1D resonant photonic crystal with different background dielectric constant in the wells $(\varepsilon_b=12.6)$ and in the barriers $(\varepsilon_0=3.0)$. In this case two different situations can be considered, namely, (i) the lattice periodicity $d=\lambda/2$ is under the Bragg condition for the exciton energy, and (ii) it is out of resonance. In Fig. 9 the photonic bands (dashed line), due to the modulation of the background dielectric constant, are shown together with the polariton curves (solid line). In an expanded scale of the dispersion curves at the boundary of the Brillouin zone (not reported here) the central and upper dispersion curves are seen not to touch. Furthermore, the photonic and polaritonic gaps do not coincide due to the contribution of the real part of the exciton susceptibility as discussed in Sec. III B.

In Fig. 10 the calculation is performed by taking the periodicity different from the Bragg condition. In this case, the normal exciton-polariton splitting is observed close to the exciton energy, but the photonic gap is moved toward the low energy side with respect to the case of background modulation due to the exciton contribution.

V. CONCLUSIONS

The self-consistent theory of the optical response for a nonlocal dispersive medium in the semiclassical framework,

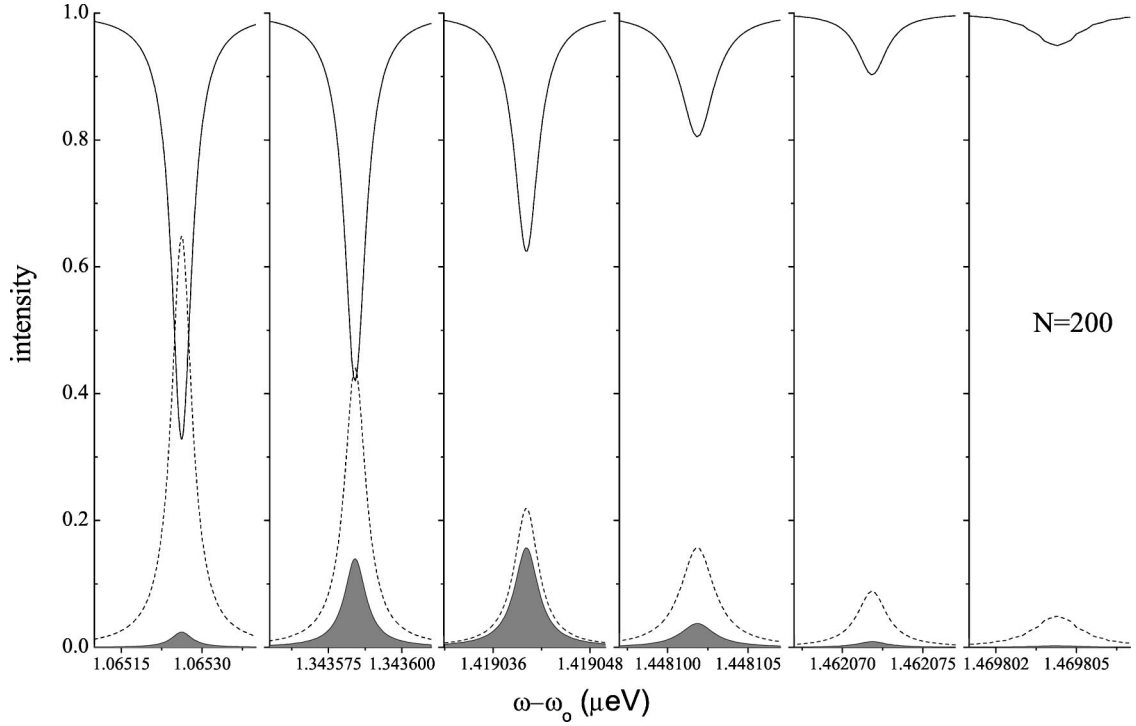

FIG. 8. Intensity of the reflectivity (straight line), transmittivity (dotted line), and absorbance (filled area) for the $N=200$ case.

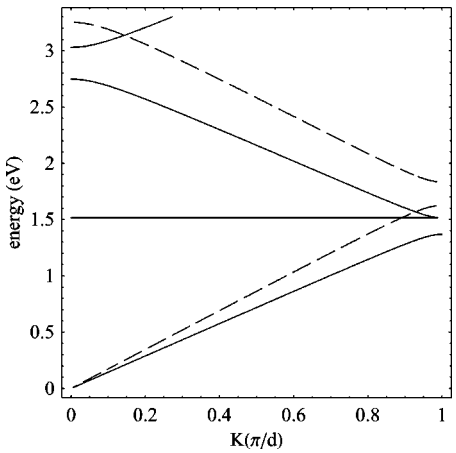

FIG. 9. Polariton dispersion curves of a 1D resonant photonic crystal of periodicity $d=(\omega_0/c)\sqrt{\varepsilon_0}$. The dashed line is the photonic curve obtained by neglecting the exciton contribution.

and the additional boundary conditions are briefly reviewed in the present paper.

The optical response of a cluster of quantum wells under the Bragg condition is studied as a function of quantum well number N from the super-radiant regime, for rather small N values, to the 1D resonant photonic crystal limit ($N\rightarrow\infty$).

The absorbance computed for a MQW system of AlGaAs/GaAs (001) shows three different behaviors, namely, (i) the super-radiant regime for a 1D cluster as large as $N\leqslant 80$, (ii) the 1D Bragg reflector behavior for $N>80$, where the radiation-matter interaction redistributes its intensity among different modes of the system; and, finally, (iii) the limit of a 1D resonant photonic system ($N\rightarrow\infty$) or very large cluster size ($N>400$), where the absorbance value becomes vanishingly small. For a deeper understanding of the light mediated interactions among the wells, we performed a decomposition of the polaritonic matrix. It has allowed us to separate in the optical response the term due to N noninteracting QWs from the interaction terms. In addition, in the interaction term two contributions has been singled out: one describing the self-interaction of the well and the other the residual interactions among different wells. Notice that the latter two contributions give the same values close to the exciton resonance for the computed system.

Finally, the polariton dispersion curves for a 1D resonant photonic crystal ($N\rightarrow\infty$) are computed, and the effects of the polariton and of the dielectric background modulation on the dispersion curves are discussed. The importance of the use of a well behaved microscopic nonlocal dielectric function for photon energy far from the resonance is pointed out using selected numerical examples.

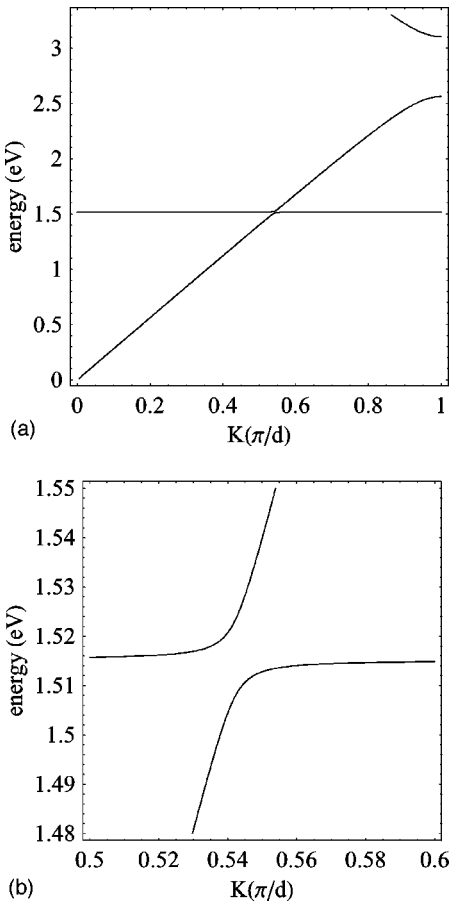

FIG. 10. (a) Polariton dispersion curves of a 1D resonant photonic crystal of periodicity $d=(\omega_0/c)\sqrt{\varepsilon_b}$. (b) Polariton curves in an expanded scale.

ACKNOWLEDGMENTS

Two of the authors (L.P. and A.D.) are indebted to the Italian MIUR FIRB Project "Nanotecnologie e nanodispositivi per la società dell'informazione" for financial support. One of the authors (K.C.) acknowledges the partial support by Grant-in-Aid for Scientific Research (No. 15540311) of the Ministry of Education, Culture, Sports, Science, and Technology of Japan.

[1] E. Yablonovich, Phys. Rev. Lett. **58**, 2059 (1987).
[2] L. Pilozzi, A. D'Andrea, and H. Fenniche, Phys. Rev. B **64**, 235319 (2001).
[3] E. L. Ivchenko, A. I. Nesvizhskii, and S. Jorda, Phys. Solid State **36**, 1156 (1994).
[4] T. Stroucken, A. Knorr, P. Thomas, and S. W. Koch, Phys. Rev. B **53**, 2026 (1995).
[5] M. Hubner, J. Kuhl, T. Stroucken, A. Knorr, S. W. Koch, R. Hey, and K. Ploog, Solid State Commun. **105**, 105 (1998).
[6] L. C. Andreani, G. Panzarini, A. V. Kavokin, and M. R. Vladimirova, Phys. Rev. B **57**, 4670 (1998).
[7] M. Hubner, J. P. Prineas, C. Ell, P. Brick, E. S. Lee, G. Khitrova, H. M. Gibbs, and S. W. Koch, Phys. Rev. Lett. **76**, 4199 (1999).
[8] G. R. Hayes, J. L. Staehli, U. Oesterle, B. Deveaud, R. T. Phillips, and C. Ciuti, Phys. Rev. Lett. **83**, 2837 (1999).
[9] M. Gurioli, M. Colocci, S. Piantelli, and S. Franchi, Phys. Status Solidi A **178**, 193 (2000).
[10] E. L. Ivchenko, Sov. Phys. Solid State **33**, 1344 (1991).

[11] L. I. Deych and A. A. Lisyansky, Phys. Rev. B **62**, 4242 (2000).
[12] T. Ikawa and K. Cho, Phys. Rev. B **66**, 085338 (2002).
[13] S. Nojima, Phys. Rev. B **59**, 5662 (1999).
[14] V. N. Piskovoi, E. F. Venger, and Y. M. Strelniker, Phys. Rev. B **66**, 115402 (2002).
[15] H. C. Schneider, F. Jahnke, S. W. Koch, J. Tignon, T. Hasche, and D. S. Chemla, Phys. Rev. B **63**, 045202 (2001).
[16] R. Matloob, R. Loudon, S. M. Barnett, and J. Jeffers, Phys. Rev. A **52**, 4823 (1995).
[17] S. I. Pekar, Zh. Eksp. Teor. Fiz. **33**, 1022 (1957) [Sov. Phys. JETP **6**, 785 (1958)]; J. J. Hopfield and D. G. Thomas, Phys. Rev. **132**, 563 (1963).
[18] C. S. Ting, M. J. Frankel, and J. L. Birman, Solid State Commun. **17**, 1285 (1975).
[19] P. Halevi and G. Hernandez-Cocoletzi, Phys. Rev. Lett. **48**, 1500 (1982).
[20] A. A. Maradudin and D. L. Mills, Phys. Rev. B **7**, 2787 (1972).
[21] A. D'Andrea and R. Del Sole, Phys. Rev. B **29**, 4782 (1984).
[22] A. Bagchi, R. G. Barrera, and A. K. Rajagopal, Phys. Rev. B **20**, 4824 (1979).
[23] A. D'Andrea and R. Del Sole, Phys. Rev. B **32**, 2337 (1985).
[24] K. Cho, J. Phys. Soc. Jpn. **55**, 4113 (1986).
[25] M. Born and E. Wolf, *Principles of Optics*, 7th ed. (Cambridge University Press, Cambridge, U.K., 1999).
[26] I. Baslev, R. Zimmermann, and A. Stahl, Phys. Rev. B **40**, 4095 (1989).
[27] K. Cho, Prog. Theor. Phys. **106**, 225 (1991).
[28] R. Atanasov, F. Bassani, A. D'Andrea, and N. Tomassini, Phys. Rev. B **50**, 14 381 (1994).
[29] E. Feenberg, Phys. Rev. **74**, 206 (1948).